Appl Phys A (2010) 99: 853–858
DOI 10.1007/s00339-010-5613-4

Applied Physics A
Materials Science & Processing

Magnetocaloric effect in antiferromagnetic Dy_3Co compound

Jun Shen · Jin-Liang Zhao · Feng-Xia Hu · Guang-Hui Rao · Guang-Yao Liu · Jian-Feng Wu · Yang-Xian Li · Ji-Rong Sun · Bao-Gen Shen

Received: 12 November 2009 / Accepted: 3 March 2010 / Published online: 16 March 2010

Abstract Magnetic properties and magnetocaloric effects (MCEs) of the Dy_3Co compound are studied. Two successive magnetic transitions: the antiferromagnetic (AFM)-to-AFM transition at $T_{AF} = 29$ K and the AFM-to-paramagnetic (PM) transition with increasing temperature at the Néel temperature $T_N = 44$ K are observed. Dy_3Co undergoes a field-induced metamagnetic transition from the AFM to the ferromagnetic (FM) state below T_N, giving rise to a large MCE. The maximal value of magnetic entropy change ΔS_m is -13.9 J/kg K with a refrigerant capacity (RC) of 498 J/kg around T_N for a field change of 0–5 T. A sign change of MCE in Dy_3Co with magnetic field and temperature is observed near the critical field where the metamagnetic transition occurs.

1 Introduction

Magnetic refrigeration technology has been demonstrated to be more environment-friendly and more efficient [1, 2] than refrigerators based on a gas compression-expansion process, but its development depends on the discovery and the synthesis of novel magnetic materials that possess large magnetocaloric effects (MCEs). Since the discovery of the large magnetic entropy change ΔS_m in $Gd_5Si_2Ge_2$ [3], there has been a great deal of interest in the study of magnetocaloric materials with a first-order phase transition, in order to obtain a large magnitude of magnetic entropy change and/or adiabatic temperature change. Many magnetic materials with the high magnetocaloric performances have been found, such as $ErCo_2$ [4], $LaFe_{13-x}Si_x$ [5, 6], $MnAs_{1-x}Sb_x$ [7], $MnFeP_{1-x}As_x$ [8], $Ni_{0.5}Mn_{0.5-x}Sn_x$ [9], etc. However, among all the magnetocaloric materials that have been investigated up to now, only a few materials, such as the paramagnetic salt $Gd_3Ga_5O_{12}$ [10] with the MCE in a low-temperature range, can be applied to magnetic refrigeration devices. Therefore, much attention has been also paid to the rare-earth (R) based intermetallic compounds with a low-temperature phase transition for the purpose of magnetic refrigerant application in recent years [11–17]. Among the R-based compounds, the R_3T (T = Co and Ni) series with the highest rare-earth content is a subject of special attention. Although these compounds have identical crystallographic structures, they exhibit complex magnetic structures and possess different magnetic-phase transitions, which will induce interesting magnetocaloric properties. Recently, the MCEs of Gd_3Co and Tb_3Co compounds have been investigated and the maximal values of magnetic entropy change ΔS_m are observed to be 11 and 18 J/kg K for a field change of 0–5 T, respectively [14, 15]. The large ΔS_m observed in Tb_3Co is found to arise from a second-order magnetic transition. The study of the magnetic properties of single crystal of Dy_3Co has revealed [18] that the compound exhibits the different AFM structures below the Néel temperature T_N and the field-induced magnetic-phase transitions along the three main axes, which are associated with a complex non-collinear AFM structure. To understand the effects of the

J. Shen (✉) · J.-F. Wu
Technical Institute of Physics and Chemistry, Chinese Academy of Sciences, Beijing 100190, People's Republic of China
e-mail: sj@g203.iphy.ac.cn

F.-X. Hu · G.-H. Rao · G.-Y. Liu · J.-R. Sun · B.-G. Shen
Beijing National Laboratory for Condensed Matter Physics and Institute of Physics, Chinese Academy of Sciences, Beijing 100190, People's Republic of China

J.-L. Zhao · Y.-X. Li
School of Material Science and Engineering, Hebei University of Technology, Tianjin 300130, People's Republic of China

AFM structure and the magnetic-phase transition, which are different from those of the R_3Co (Gd and Tb) compounds, on magnetocaloric behaviour, we study the magnetic properties and the MCEs of Dy_3Co compound in the present paper. The MCE is observed to change its sign with temperature and/or applied magnetic field, which results from the field-induced metamagnetic transition from AFM to FM state below T_N. A large reversible MCE with a considerable refrigerant capacity around T_N is obtained in Dy_3Co.

2 Experimental procedures

Polycrystalline Dy_3Co was prepared by arc melting in a high-purity argon atmosphere. The purities of starting materials were 99.9% for Dy and Co. The sample was turned over and remelted several times to ensure its homogeneity. The ingot obtained by arc melting was wrapped by molybdenum foil, sealed in a quartz tube of high vacuum, annealed at 873 K for 8 days and then quenched to room temperature. X-ray diffraction (XRD) measurements on powder samples were performed by using Cu Kα radiation to identify the crystal structure. Magnetizations were measured as functions of temperature and magnetic field by using a superconducting quantum interference device (SQUID) magnetometer. Both the ac susceptibility and the specific heat were measured by using a physical property measurement system (PPMS) from Quantum Design.

3 Results and discussion

Figure 1 shows the Rietveld refined powder XRD patterns of Dy_3Co compound at room temperature. The refinement shows that the prepared sample is of single phase, crystalliz-

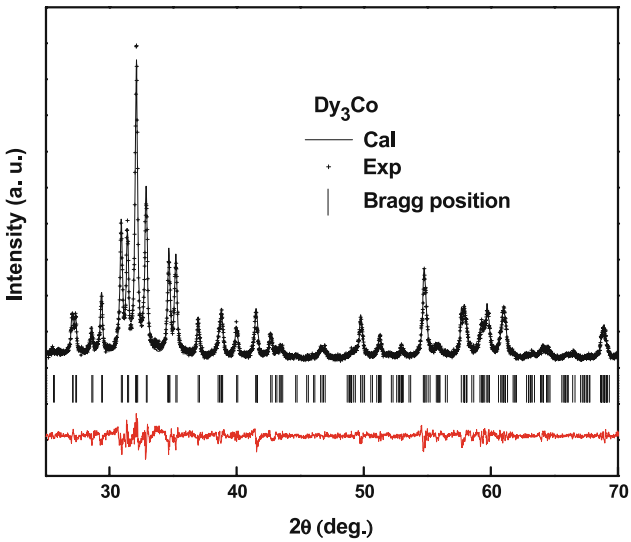

Fig. 1 Rietveld refined powder XRD patterns of Dy_3Co compound at room temperature. The observed data are indicated by *crosses* and the calculated profile is the *continuous line* overlying them. The *short vertical lines* indicate the angular positions of the Bragg peaks of Dy_3Co. The lower curve is the difference between the observed and calculated intensity

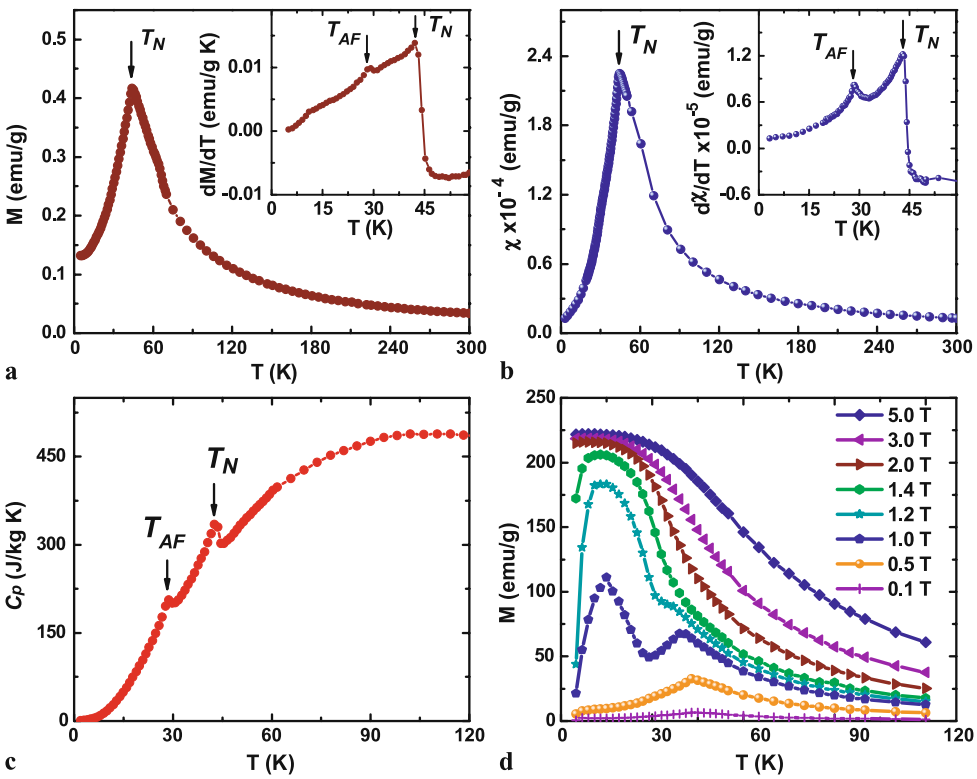

Fig. 2 Temperature dependences of magnetization under a magnetic field of 0.01 T (**a**), ac susceptibility for a constant frequency of 1000 Hz (**b**) and zero-field specific heat (**c**) for Dy_3Co. We see the temperature dependence of the magnetization at different magnetic fields (**d**). The *insets* in (**a**) and (**b**) show the dM/dT–T and $d\chi/dT$–T curves, respectively

ing in the orthorhombic Fe_3C type crystal structure (space group Pnma). The lattice parameters are determined to be $a = 6.977(3)$ Å, $b = 9.321(4)$ Å and $c = 6.241(2)$ Å by using the Rietveld refinement method, which is almost in accord with those in the previous report [18].

Figures 2(a), (b) and (c) show the temperature (T) dependences of the magnetization (M) in a magnetic field of 0.01 T, the ac susceptibility (χ) for a constant frequency of 1000 Hz and the specific heat (C_p) in a zero-field for Dy_3Co, respectively. The results in Fig. 2 show that Dy_3Co has two successive magnetic transitions as reported by Baranov et al. previously [18]. The anomaly at lower temperature may be associated with the phase transition from one AFM to another AFM state [18]. The transition temperature ($T_{AF} = 29$ K), determined by the position of the low-temperature peak on the specific heat curve, is fully consistent with the value derived from the dM/dT–T and $d\chi/dT$–T curves (see the inset of Fig. 2(a) and (b), respectively). The transition at higher temperature corresponds to a change from AFM to PM state as temperature increases. The Néel temperature T_N is determined to be 44 K, which is in good agreement with the previous results [18, 19]. Figure 2(d) shows the temperature dependence of the magnetization at different magnetic fields. It is clearly observed that the magnetic fields can drive magnetic transition temperatures T_{AF} and T_N to lower temperature and a field-induced metamagnetic transition from AFM to FM state is present below T_N. When the applied magnetic field is higher than about 1.2 T, the magnetization as a function of temperature for Dy_3Co exhibits steplike behavior above T_N, which corresponds to the FM to PM transition. A similar result has been observed in DySb [20].

Figure 3(a) shows the isothermal magnetization curves of Dy_3Co in a temperature range of 5–120 K under the magnetic fields up to 5 T. The temperature steps are chosen to be 2, 5 and 10 K in temperature ranges of 5–55 K, 55–100 K and 100–120 K, respectively. The magnetization of Dy_3Co below T_N is found to increase linearly with increasing magnetic field in low-field ranges (see Fig. 3(b)), indicating the existence of AFM ground state. However, it is found that the magnetization exhibits a sharp increase when the applied field exceeds a certain value, indicating that the field-induced metamagnetic transition from AFM to FM state occurs. The critical field required for metamagnetism for Dy_3Co, which is determined from the maximum of dM/dH, is found first to decrease with the increase of temperature, passing through a minimum value of 1.0 T at about 15 K, and then to increase again with increasing temperature. One can also find from Fig. 3(a) that the magnetization of Dy_3Co is easily saturated below T_N above the critical field due to the field-induced FM state and its magnitude gradually decreases with the increase of temperature. For temperatures much higher than T_N, the field dependence of the magnetization shows a linear relation. However, the isothermal magnetization curves obtained well above T_N show an appreciable non-linearity. The curvature in the M–H curves probably indicates the existence of short-range ferromagnetic correlations in the paramagnetic state. Similar results have been observed in many other intermetallic compounds [21–23].

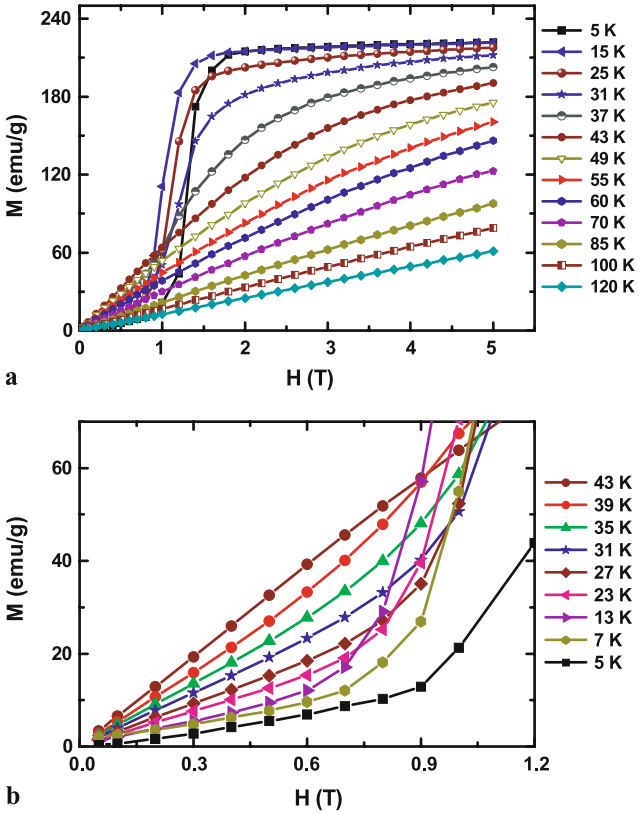

Fig. 3 Isothermal magnetization curves of Dy_3Co in a temperature range of 5–120 K (**a**), magnetization curves below T_N in a low magnetic-field region of 0–1.2 T (**b**)

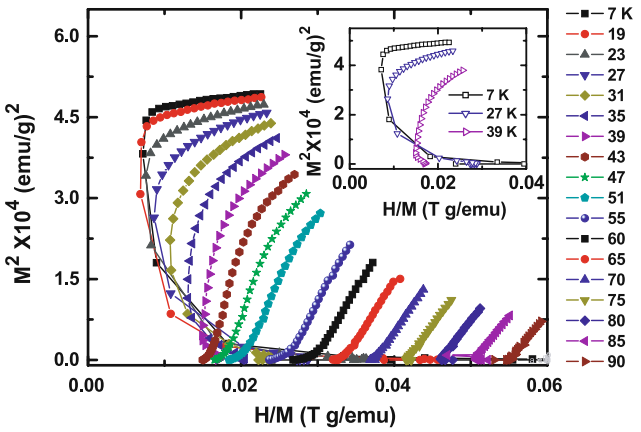

Fig. 4 Arrott plots of Dy_3Co at different temperatures. The *inset* shows the Arrott curve at 7, 27 and 39 K

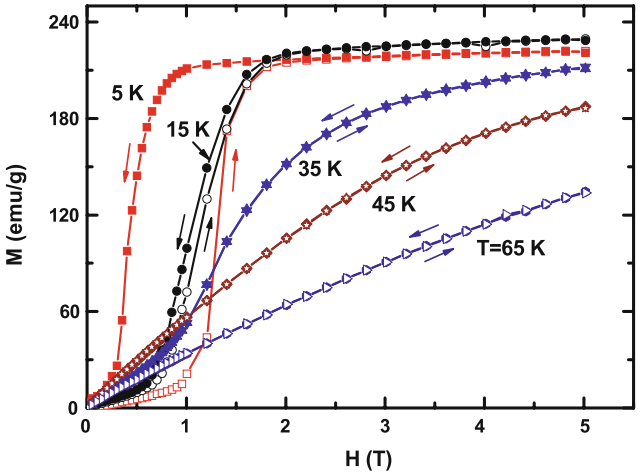

Fig. 5 Magnetization curves of Dy_3Co under increasing and decreasing fields at temperatures of 5, 15, 35, 45 and 65 K, respectively

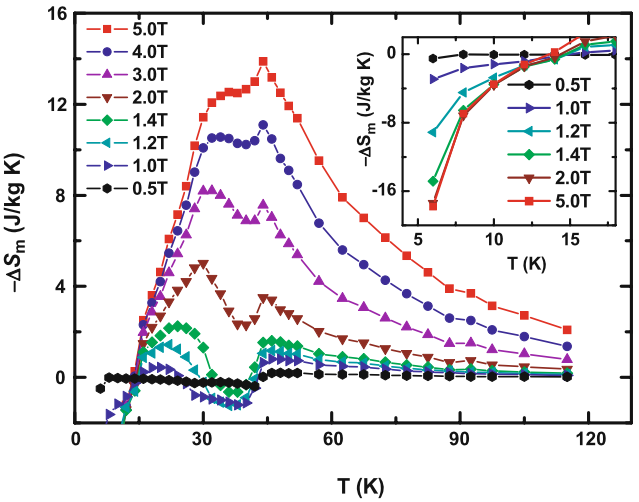

Fig. 6 Temperature dependences of magnetic entropy change $-\Delta S_m$ for the Dy_3Co compound for different magnetic-field changes. The *inset* shows the temperature dependences of $-\Delta S_m$ in a low-temperature range of 5–18 K

The Arrott plots of Dy_3Co compound at different temperatures are shown in Fig. 4. According to the Banerjee criterion [24], a magnetic transition is expected to be of the first order when the slope of the Arrott plot is negative, whereas it will be of the second order when the slope is positive. The criterion of the Arrott plot has been successfully used to describe the essence of disorder-order phase transitions between PM and FM states [25] and in the order-order AFM-to-FM transition [20, 26]. It can be clearly seen from the inset of Fig. 4 that the negative slope of the Arrott plot for Dy_3Co below T_N confirms the first-order AFM-to-FM transition. However, the positive slope above T_N indicates the characteristic of a field-induced second-order PM-to-FM transition.

The magnetization curves for Dy_3Co under increasing and decreasing fields exhibit an obvious magnetic hysteresis loop at low temperatures as shown in Fig. 5, due to the field-induced first-order phase transition. The hysteresis loss, defined as the area enclosed by the ascending and descending branches of magnetization curve, is found to be 179 J/kg at 5 K, and decreases rapidly to a small value of 19 J/kg at 15 K. Above ~20 K, the magnetization curves under increasing and decreasing fields are completely reversible and no magnetic hysteresis is observed. This is very favorable for magnetic refrigeration.

In an isothermal process of magnetization, the magnetic entropy change of the materials can be derived from the Maxwell relation by integrating the magnetization M over the magnetic field H, i.e.

$$\Delta S_m(T,H) = S_m(T,H) - S_m(T,0) = \int_0^H \left(\frac{\partial M}{\partial T}\right)_H dH. \tag{1}$$

To derive the temperature dependence of magnetic entropy change, the following numerical approximation of the integral is usually adopted under increasing and decreasing fields:

$$|\Delta S_m| = \sum_i \frac{M_i - M_{i+1}}{T_{i+1} - T_i} \Delta H_i, \tag{2}$$

where M_i and M_{i+1} are the experimental values of the magnetization measured at T_i and T_{i+1} in an applied magnetic field H_i, respectively. For Dy_3Co, we calculate the ΔS_m associated with the H variation according to expression (2). Figure 6 shows the values of ΔS_m as a function of temperature for different magnetic field changes up to $H = 5$ T, which give some valuable information about the physical essence of the magnetic ordering in Dy_3Co. The negative values of ΔS_m in the FM and the PM states result from a magnetically more ordered configuration with the application of an external magnetic field [27]. However, the positive value of ΔS_m in the AFM ordering is due to disordered magnetic sublattices antiparallel to the applied magnetic field [26]. It is observed from Fig. 6 that the values of ΔS_m of Dy_3Co are positive at temperatures below ~15 K, but they change to a negative value with the increase of temperature due to the field-induced magnetic transition from AFM to FM state. A large positive value of ΔS_m is observed to be 17.8 J/kg K at 5 K for a field change of 0–5 T as shown in the inset of Fig. 6, indicating a strong dominance of AFM ordering at low temperatures. However, the ΔS_m value estimated by the Maxwell relation at low temperature may be in error due to the field-induced metamagnetic transition, which leads to a large magnetic hysteresis. The actual ΔS_m values below ~15 K should be lower than the estimated values. It can be also seen from Fig. 6 that the value of ΔS_m around T_{AF} is also positive

Table 1 Curie temperature T_C or Néel temperature T_N, magnetic entropy change ΔS_m and refrigerant capacity RC under a magnetic-field change of 0–5 T for some magnetocaloric materials with a magnetic ordering temperature of about 44 K

Materials	T_C or T_N (K)	$-\Delta S_m$ (J/kg K)	RC (J/kg)	Refs.
TbNiAl	47	13.8	494	[12]
$Gd_{0.7}Er_{0.3}NiAl$	~40	11	505[a]	[32]
GdNiAl	40	12	540[a]	[33]
$ErCo_2$	35	33	270[a]	[34]
$Er(Co_{0.975}Si_{0.025})_2$	41	27.4	260[a]	[34]
$Ho(Co_{0.9}Ni_{0.1})_2$	40	22	330[a]	[35]
$NdAl_2$	36	7.6	90[a]	[17]
$GdAl_2$	44	7.2	290[a]	[17]
$Pr_6Co_{1.67}Si_3$	48	6.9	200[a]	[13]
Dy_3Co	44	13.9	498	This work

[a]The RC values are estimated from the temperature dependence of ΔS_m in the literatures, respectively

for small magnetic-field changes because of the presence of the AFM state, but it becomes negative for fields larger than the critical field due to the field-induced FM state. When the temperature is increased to T_N, the field-induced AFM-to-FM transition leads again to a large negative ΔS_m. Such a sign change of MCE with magnetic field and/or temperature in Dy_3Co is different from the case in isostructural R_3Co (R = Gd and Tb) [14, 15]. The positive ΔS_m (negative MCE) is often observed in magnetocaloric materials with the first-order magnetic transitions [28, 29], which results from the mixed exchange interaction, and the applied magnetic field leads to a further spin-disordered state near the transition temperature, thereby increasing the configurational entropy [20, 30]. It is clearly observed from Fig. 6 that the ΔS_m–T curves of Dy_3Co exhibit two maximum values at ~29 and 44 K, respectively, which corresponds to the two transitions at T_{AF} and T_N in the M–T curves. The maximum value of ΔS_m for Dy_3Co is found to be −13.9 J/kg K around T_N for a magnetic-field change from 0 to 5 T. It is apparent that the large ΔS_m in Dy_3Co is associated with the field-induced metamagnetic transition below T_N. The refrigerant capacity (RC) of Dy_3Co compound has been also calculated by numerically integrating the area under the ΔS_m–T curve (Fig. 6), with the temperatures at half maximum of the peak used as the integration limits [31]. The RC value thus obtained for Dy_3Co is 498 J/kg with $T_{\text{cold}} = 23.5$ K (temperature of the cold reservoir) and $T_{\text{hot}} = 68.5$ K (temperature of the hot reservoir) for a field changing from 0 to 5 T. The large RC originates from the combined contribution of two successive magnetic transitions, which enlarge the temperature span of large MCE. The full width at half maximum of the ΔS_m peak under a magnetic field of 5 T attains $\Delta T = 45$ K ($\Delta T = T_{\text{hot}} - T_{\text{cold}}$) for Dy_3Co due to the superposition of the AFM-to-AFM and AFM-to-PM phase transitions. For comparison, the magnetocaloric properties of our sample and some magnetocaloric materials with a similar magnetic ordering temperature are listed in Table 1. It is found that both the ΔS_m and RC for Dy_3Co are comparable to those of TbNiAl [12], (Gd, Er)NiAl [32] compounds and amorphous GdNiAl alloy [33]. Although the $ErCo_2$ compound, which undergoes the itinerant-electron metamagnetic transition, exhibits a large ΔS_m around the Curie temperature of ~35 K [34], its RC value is much smaller than that of Dy_3Co due to the peak in the ΔS_m–T curves of $ErCo_2$ being relatively narrow. Large ΔS_m and small RC values are also observed in $Er(Co_{0.975}Si_{0.025})_2$ [34] and $Ho(Co_{0.9}Ni_{0.1})_2$ [35] compounds (Table 1). It can also be seen from Table 1 that the values of ΔS_m and RC for Dy_3Co are also much larger than those of $Pr_6Co_{1.67}Si_3$ [13] and RAl_2 (R = Nd and Gd) [17] compounds. Therefore, the large ΔS_m and the considerable RC values around T_N as well as there being no magnetic hysteresis (above ~20 K) in Dy_3Co are very useful for its application in magnetic refrigeration.

4 Conclusions

In summary, it is found that Dy_3Co has two successive magnetic transitions: the AFM-to-AFM transition at $T_{AF} = 29$ K and the AFM-to-PM transition at $T_N = 44$ K. The compound undergoes a field-induced metamagnetic transition from AFM to FM state below T_N. A sign change from the negative MCE to the positive MCE near the critical field with the increase of magnetic field or temperature are observed in the Dy_3Co compound below T_N. The large MCE in Dy_3Co is found to be associated with the field-induced metamagnetic transition. The maximal value of ΔS_m is −13.9 J/kg K with a considerable RC value of 498 J/kg around T_N for a field change of 0–5 T. The large reversible

ΔS_m as well as the considerably reversible RC suggests that Dy_3Co may be an appropriate candidate for magnetic refrigerant in low-temperature ranges.

Acknowledgements The present work was supported by the National Basic Research Program of China, the National Natural Science Foundation of China and the Knowledge Innovation Project of the Chinese Academy of Sciences.

References

1. K.A. Gschneidner Jr., V.K. Pecharsky, A.O. Tsokol, Rep. Prog. Phys. **68**, 1479 (2005)
2. C.B. Zimm, A. Jastrab, A. Sternberg, V.K. Pecharsky, K.A. Gschneidner Jr., M. Osborne, I. Anderson, Adv. Cryog. Eng. **43**, 1759 (1998)
3. V.K. Pecharsky, K.A. Gschneidner Jr., Phys. Rev. Lett. **78**, 4494 (1997)
4. A. Giguere, M. Foldeaki, W. Shcnelle, E. Gmelin, J. Phys., Condens. Matter **11**, 6969 (1999)
5. F.X. Hu, B.G. Shen, J.R. Sun, Z.H. Chen, G.H. Rao, X.X. Zhang, Appl. Phys. Lett. **78**, 3675 (2001)
6. B.G. Shen, J.R. Sun, F.X. Hu, H.W. Zhang, Z.H. Cheng, Adv. Mater. **21**, 4545 (2009)
7. H. Wada, Y. Tanabe, Appl. Phys. Lett. **79**, 3302 (2001)
8. O. Tegus, E. Brück, K.H.J. Buschow, F.R. de Boer, Nature (London) **415**, 150 (2002)
9. T. Krenke, E. Duman, M. Acet, E.F. Wassermann, X. Moya, L. Mañosa, A. Planes, Nat. Mater. **4**, 450 (2005)
10. J.A. Barclay, W.A. Steyert, Cryogenics **22**, 73 (1982)
11. X.X. Zhang, F.W. Wang, G.H. Wen, J. Phys., Condens. Matter **13**, L747 (2001)
12. N.K. Singh, K.G. Suresh, R. Nirmala, A.K. Nigam, S.K. Malik, J. Magn. Magn. Mater. **302**, 302 (2006)
13. J. Shen, F. Wang, Y.X. Li, J.R. Sun, B.G. Shen, J. Alloys Compd. **458**, L6 (2008)
14. S.K. Tripathy, K.G. Suresh, A.K. Nigam, J. Magn. Magn. Mater. **306**, 24 (2006)
15. B. Li, J. Du, W.J. Ren, W.J. Hu, Q. Zhang, D. Li, Z.D. Zhang, Appl. Phys. Lett. **92**, 242504 (2008)
16. B. Li, W.J. Hu, X.G. Liu, F. Yang, W.J. Ren, X.G. Zhao, Z.D. Zhang, Appl. Phys. Lett. **92**, 242508 (2008)
17. P. Kumar, K.G. Suresh, A.K. Nigam, J. Phys. D, Appl. Phys. **41**, 105007 (2008)
18. N.V. Baranov, A.N. Pirogov, A.E. Teplykh, J. Alloys Compd. **226**, 70 (1995)
19. N.V. Baranov, E. Bauer, R. Hauser, A. Galatanu, Y. Aoki, H. Sato, Eur. Phys. J. B **16**, 67 (2000)
20. W.J. Hu, J. Du, B. Li, Q. Zhang, Z.D. Zhang, Appl. Phys. Lett. **92**, 192505 (2008)
21. N.K. Singh, K.G. Suresh, R. Nirmala, A.K. Nigam, S.K. Malik, J. Appl. Phys. **101**, 093904 (2007)
22. R. Mallik, E.V. Sampathkumaran, P.L. Paulose, Solid State Commun. **106**, 169 (1998)
23. P. Arora, P. Tiwari, V.G. Sathe, M.K. Chattopadhyay, J. Magn. Magn. Mater. **321**, 3278 (2009)
24. S.K. Banerjee, Phys. Lett. **12**, 16 (1964)
25. H. Saito, T. Yokoyama, K. Fukamichi, J. Phys., Condens. Matter **9**, 9333 (1997)
26. T. Samanta, I. Das, S. Banerjee, Appl. Phys. Lett. **91**, 152506 (2007)
27. T. Samanta, I. Das, Phys. Rev. B **74**, 132405 (2006)
28. M.P. Annaorazov, S.A. Nikitin, A.L. Tyurin, K.A. Asatryan, A.K. Dovletov, J. Appl. Phys. **79**, 1689 (1996)
29. O. Tegus, E. Brück, L. Zhang, Dagula, K.H.J. Buschow, F.R. de Boer, Physica B **319**, 174 (2002)
30. T. Krenke, E. Duman, M. Acet, E.F. Wassermann, X. Moya, L. Manosa, A. Planes, Nat. Mater. **4**, 450 (2005)
31. K.A. Gschneidner Jr., V.K. Pecharsky, A.O. Pecharsky, C.B. Zimm, Mater. Sci. Forum **315–317**, 69 (1999)
32. B.J. Korte, V.K. Pecharsky, K.A. Gschneidner Jr., J. Appl. Phys. **84**, 5677 (1998)
33. L. Si, J. Ding, Y. Li, B. Yao, H. Tan, Appl. Phys. A **75**, 535 (2002)
34. N.K. Singh, P. Kumar, K.G. Suresh, A.K. Nigam, A.A. Coelho, S. Gama, J. Phys., Condens. Matter **19**, 036213 (2007)
35. T. Tohei, H. Wada, J. Magn. Magn. Mater. **280**, 101 (2004)